

Breakdown of the Stokes-Einstein Relation Above the Melting Temperature in a Liquid Phase-Change Material

Shuai Wei¹, Zach Evenson^{2*}, Moritz Stolpe³, Pierre Lucas⁴, C. Austen Angell^{5*}

¹*Institute of Physics (IA), RWTH Aachen University, Aachen, Germany*

²*Maier-Leibnitz Zentrum (MLZ) and Physik Department, Technische Universität München, Lichtenbergstrasse 1, 85747 Garching, Germany*

³*Heraeus Holding GmbH, Germany*

⁴*Department of Materials Science and Engineering, University of Arizona, Tucson, Arizona 85712, United States.*

⁵*School of Molecular Sciences, Arizona State University, Tempe, Arizona 85287, United States.*

ABSTRACT

The dynamic properties of liquid phase-change materials (PCMs), such as viscosity η and atomic self-diffusion coefficients D , play an essential role in ultrafast phase switching behavior of novel non-volatile phase-change memory applications, as they are intimately related to crystallization kinetics and phase stabilities. To connect η to D , the Stokes-Einstein relation (SER) is commonly assumed to be valid at high temperatures near or above the melting temperature T_m and is frequently employed for assessing liquid fragility (or crystal growth velocity) of technologically important PCM compositions. However, using quasi-elastic neutron scattering (QENS), we give here experimental evidence for a breakdown of the SER even at temperatures above T_m in the high-atomic-mobility state of a typical PCM, $\text{Ge}_1\text{Sb}_2\text{Te}_4$, where the decay of density correlation functions still remains exponential. The origin of the breakdown is thus unlikely the result of dynamical heterogeneities, as is usually postulated for viscous liquids. Rather, we discuss its possible connections to a metal-semiconductor and fragile-strong transition hidden below T_m .

INTRODUCTION

PCMs can be reversibly switched between their glassy and crystalline states by heating with a voltage or laser pulse(I). The strong optical/electrical contrast between these two states makes PCMs highly interesting for data storage applications (e.g. encoding “0” and “1”). An extremely fast phase switching on a time-scale of nanoseconds is a requirement for fast read/write speed. However, the fast atomic dynamics inherent to PCMs seems to be at odds with the concomitant requirement of good amorphous phase stability for data retention(I). Typical PCMs include the Ge-Sb-Te alloys, especially those along the GeTe - Sb_2Te_3 tie line, and doped Sb_2Te_3 alloys such

*Corresponding authors. Email: austenangell@gmail.com (C.A.A.), zachary.evenson@frm2.tum.de (Z.E.).

as Ag-In-Sb-Te(2). Physical understanding of PCMs has been mainly centered around features of their crystalline states (e.g. bonding(3) and vacancy ordering(4)), while the liquid-state behavior was considered ‘ordinary’ or less explored, probably because a large portion of the (supercooled) liquid state is obscured by fast crystallization.

Requiring a critical cooling rate of $\sim 10^{10}$ K s⁻¹ for vitrification, PCMs are generally recognized as poor glass formers. In fact, the amorphous phase is so prone to crystallization that no glass transition (T_g) can be observed in a differential scanning calorimeter (DSC)(5) before crystallization sets in upon heating(6). Thus, the broad supercooled liquid regime, $\Delta T = T_m - T_x$, between the melting temperature (e.g. $T_m \sim 903$ K for Ge₁Sb₂Te₄) and the crystallization temperature upon heating (typically $T_x \sim 400$ K for GeTe - Sb₂Te₃ alloys) is experimentally inaccessible using standard techniques. For this reason, it has been a long-standing challenge to characterize the liquid-state behavior of PCMs -- specifically, the liquid fragility that has been recently given much importance by Greer and coworkers(7). The latter, defined as $m = d \log \eta / d(T_g/T) |_{T=T_g}$, where T_g is the “standard” value (where the viscosity η reaches the value 10¹² Pa·s)(8), describes the deviation of the temperature-dependence of viscosity from the Arrhenius law. Fragility has been recognized as a useful parameter for understanding crystallization kinetics and the stability of amorphous states(9, 10).

The SER is frequently employed to calculate η from D (or vice-versa) in technologically important PCMs at ‘sufficiently’ high temperature,

$$D \cdot \eta = (k_B \cdot T) / (6\pi r_H), \quad (1)$$

where k_B is the Boltzmann constant, T the absolute temperature, and r_H the effective hydrodynamic radius. For instance, Orava et al.(7) assumed a valid SER at T_m for deriving the absolute values of crystal growth velocity of Ge₂Sb₂Te₅ from the Kissinger-type analysis using ultrafast DSC data. Salinga et al.(11) used crystal growth velocity data from laser reflectivity measurements for determining the fragility of Ag-In-Sb-Te ($m \sim 190$), assuming a valid SER over a wide temperature range well below T_m . Schumacher et al.(12) compared the experimental viscosity data for Ge₂Sb₂Te₅ at $T > T_m$ to the values derived from the SER based on simulated self-diffusion coefficients, and observed a non-negligible discrepancy.

In general, liquids at high temperature are expected to obey the SER, as they do not feel the energy landscape and single-particle dynamics follow the same temperature-dependence as the collective macroscopic stress relaxation processes. When the temperature approaches T_g on

cooling, D progressively decouples from η in fragile liquids such as o-terphenyl (OTP), PDE, and salol, beginning at $\sim 1.2T_g$ (ref.(13)), supposedly due to the dynamic heterogeneity(13). A SER breakdown in PCM GeTe was also asserted by Sosso et al.(14) based on ab initio simulations, which occurs in the supercooled liquid attributed to dynamic heterogeneities. Such a breakdown in supercooled $\text{Ge}_2\text{Sb}_2\text{Te}_5$ and GeTe nanoparticles was also taken into account by Chen et al. (15) and Orava et al.(7), where the necessity of using a fractional SER to describe the supercooled liquid, was emphasized. Also, the crystal growth kinetic coefficient U_{kin} decouples from η following the Ediger et al relation(9) $U_{kin} \propto \eta^{\zeta^*}$ ($\zeta^* < 1$ depending on fragility). Detailed experimental studies of multi-component bulk metallic glass-forming liquids with high atomic packing fractions(16) ($\varphi \sim 0.51-0.55$) revealed a clear breakdown of the SER close to, or even well above, the critical temperature T_c of mode-coupling theory (MCT)(17–19). Liquid PCMs, on the other hand, represent p -electron bonded(20, 21) fragile glass formers(7, 22) with low atomic packing fractions ($\varphi \sim 0.3-0.4$). There has been surprisingly little interest in, or experimental data related to, the SER above T_m for PCMs. However, the recent discussion concerning the likely existence of liquid-liquid transitions (LLTs) in PCMs suggests the probability of complex dynamical behavior, including a breakdown of the SER in these liquids(23).

In this work, we probe the microscopic dynamics in the liquid state of a typical PCM $\text{Ge}_1\text{Sb}_2\text{Te}_4$ using QENS, which permits direct determination of both the structural α -relaxation time, (proportional to shear viscosity η), and the self-diffusion coefficient D on the same sample under identical conditions. Our results question the validity of the commonly employed SER in those technologically important PCMs, even well above T_m . We discuss the origin of the breakdown of SER and its relation to a possible metal-semiconductor and fragile-strong transition hidden below T_m , which may play a critical role in speeding up crystallization kinetics, before restraining the atomic rearrangements through a fragile-to-strong transition. The fundamental importance of such phenomena to the technical performance of PCMs has been stressed elsewhere(23, 24).

RESULTS

α -relaxation time

We obtain relaxation times from the decay of the intermediate scattering function (ISF) $S(q,t)$ which describes the decay of microscopic density fluctuations in the liquid and was obtained according to the procedure outlined in the Materials and Methods. Figure 1a shows $S(q,t)$ taken at the first structure factor maximum $q_0=2.0 \text{ \AA}^{-1}$ of the liquid at different temperatures above $T_m=903$

K. The data are best fitted with a simple exponential function, $S(q,t)/S(q,0) = f_q \exp(-t/\tau_q)$, where f_q is a constant accounting for atomic vibrations and τ_q is the structural relaxation time. In the case of $q_0=2.0 \text{ \AA}^{-1}$, i.e. the position of the structure factor maximum, the fitting yields a collective structural relaxation time, or α -relaxation time τ_α , shown in Figure 1b, as the quasi-elastic signal at q_0 arises predominantly from the coherent scattering contribution. τ_α is associated with the shear viscosity η in the viscoelastic model of Maxwell, which establishes a proportional relation via $\eta = G_\infty \cdot \tau_\alpha$, where G_∞ is the infinite-frequency shear modulus measured on time scales very short with respect to τ_α . This proportionality has been directly tested by combining QENS and viscosity measurements on various glass forming melts(18, 25, 26).

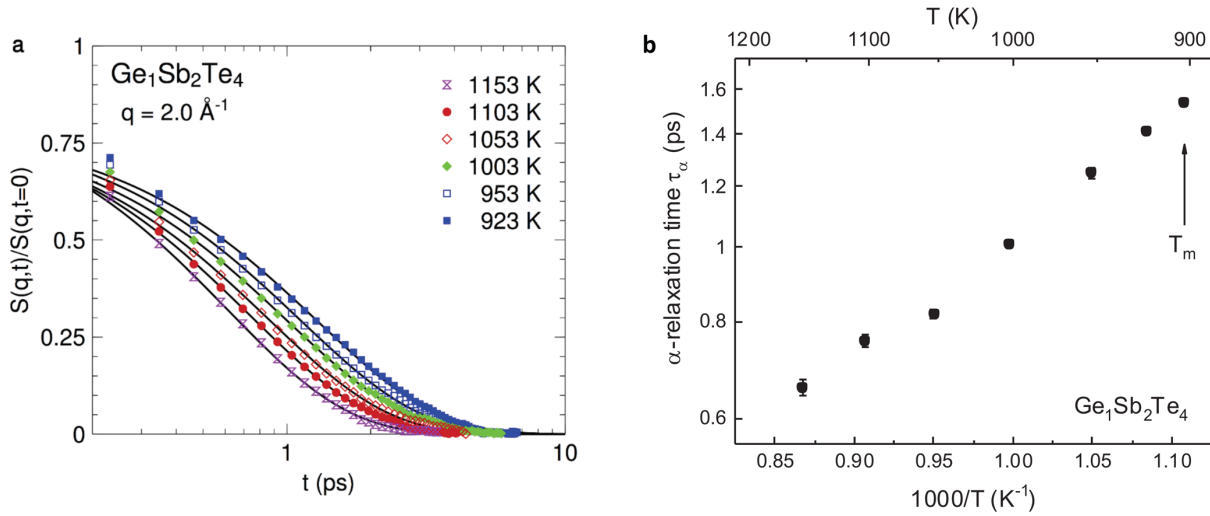


Figure 1. Exponential decay of the ISF and the α -relaxation time τ_α for liquid $\text{Ge}_1\text{Sb}_2\text{Te}_4$ above T_m . (a) The decay of the ISF $S(q,t)$ of liquid $\text{Ge}_1\text{Sb}_2\text{Te}_4$ at the structure factor first maximum $q_0=2.0 \text{ \AA}^{-1}$ measured at temperatures above $T_m=903 \text{ K}$. The data, typical of high fluidity systems, are best fitted by simple exponential functions (solid lines), each yielding a single relaxation time τ_α (see text for details). Note that at very short time ($<0.65 \text{ ps}$) the data points correspond to phonons and fast processes that are not explicitly taken into account in the fitting. This is consistent with the analysis of the dynamic structure factor $S(q, \omega)$ in the energy transfer ($\hbar\omega$) domain (see SI-Fig.S1), where $S(q, \omega)$ is best described by a single Lorentzian form. (b) Arrhenius plot for the α -relaxation time τ_α above T_m .

Self-diffusivity

Self-diffusion coefficients were determined from the QENS signal in the low- q range, where the signal is dominated by the incoherent scattering of both Ge and Te atoms and reflects their single-particle dynamics on long length and time scales. Given the incoherent cross-sections of each

species and their relative concentration in the alloy melt, the measured self-diffusion coefficient of $\text{Ge}_1\text{Sb}_2\text{Te}_4$ represents a mean value weighted by roughly 1/3 Ge and 2/3 Te. As shown in the inset of Fig. 2, the incoherent relaxation times τ^{inc} indeed follow a $1/q^2$ dependence at low $q^2 \leq 0.6 \text{ \AA}^{-2}$, which is characteristic of long-range atomic diffusion in liquids in the hydrodynamic limit as $q \rightarrow 0 \text{ \AA}^{-1}$ (ref.(27)). This thus allows us to derive a mean Ge/Te self-diffusion coefficient via $D_{\text{Ge/Te}} = 1/(\tau^{inc} q^2)$. In Figure 2, the resulting $D_{\text{Ge/Te}}$ are fitted with the Arrhenius law, yielding an activation energy $E_{a,D} = 26.41 \pm 0.89 \text{ kJ mol}^{-1}$ and a pre-exponent $D_0 = 1.4 \times 10^{-7} \text{ m}^2 \text{ s}^{-1}$. To our knowledge, there are no experimental diffusivity data available for liquid PCMs. Some partial atomic diffusion coefficients are available from *ab initio* computer simulations (28) $D_{\text{Ge}} = 4.04 \times 10^{-9} \text{ m}^2 \text{ s}^{-1}$, and $D_{\text{Te}} = 4.06 \times 10^{-9} \text{ m}^2 \text{ s}^{-1}$ at 1000 K for the same composition, which are close to our value ($D \approx 5.7 \times 10^{-9} \text{ m}^2 \text{ s}^{-1}$) at 1003 K.

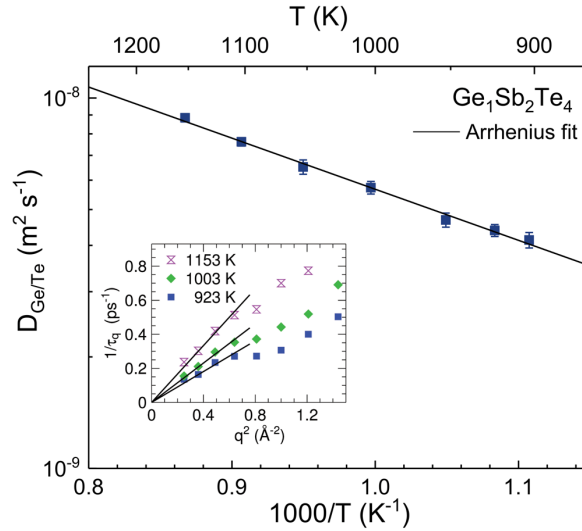


Figure 2. Mean self-diffusion coefficient $D_{\text{Ge/Te}}$ of liquid $\text{Ge}_1\text{Sb}_2\text{Te}_4$ derived from incoherent scattering signal at low q . Inset: q^2 -dependence of the inverse relaxation time $1/\tau_q$. At low- q ($q^2 \leq 0.6 \text{ \AA}^{-2}$), $1/\tau_q$ follows a q^2 -dependence (solid straight lines), as expected from hydrodynamic theory as $q \rightarrow 0 \text{ \AA}^{-1}$. For $q^2 > 0.6 \text{ \AA}^{-2}$, $1/\tau_q$ deviates from the q^2 -dependence due to coherent scattering contributions from a pre-peak of $S(q)$ at $\sim 1 \text{ \AA}^{-1}$ (see SI-Fig.S3).

DISCUSSION

According to the SER, the product $(D \cdot \eta)/T$ and, hence, $(D \cdot \tau_a)/T$ should remain constant as a function of T [Eq. (1)]. For the liquid PCM $\text{Ge}_1\text{Sb}_2\text{Te}_4$, this is evidently not the case, as highlighted in Figure 3a. This relation appears to hold at high temperatures ($T \gtrsim 1050 \text{ K}$). However, a marked deviation is observed at 1050 K on approaching T_m (903 K) during cooling, indicating a breakdown

of the SER well above the melting point, $T_{SE} = 1.16T_m$. Note that we take the SER in its form of $D \propto (\tau_\alpha/T)^{-1}$. If G_∞ in the Maxwell relation is temperature dependent (as it certainly is for fragile liquids), then the temperature of SER breakdown, in its original form with viscosity, might differ somewhat from the breakdown temperature observed here. In either case it should occur at relaxation times of order 1ps (from Fig. 1 and Fig 3b), far shorter than in any normal liquid where the breakdown only occurs at nanosecond relaxation times.

In Fig.3b, by fitting the data with a fractional SER of the form(29),

$$D \propto (\tau_\alpha/T)^{-\xi}, \quad (2)$$

where $0 < \xi \leq 1$, we see that the high-temperature liquid for $T \geq 1050$ K indeed closely follows the SER with an exponent $\xi \approx 0.97 \pm 0.11$, while $\xi \approx 0.60 \pm 0.03$ is obtained for $T \leq 1050$ K, indicating a strong deviation from the SER. The latter is related to the decoupling of crystal growth coefficient U_{kin} and viscosity η for fragile liquids, which is described by the form $U_{kin} \propto \eta^{-\xi^*}$ given by Ediger et al.(9). Indeed, $\xi^* = 0.67$ in a similar PCM $\text{Ge}_2\text{Sb}_2\text{Te}_5$, estimated by Orava et al.(7) from an empirical correlation with fragility, is close to our $\xi \approx 0.6$.

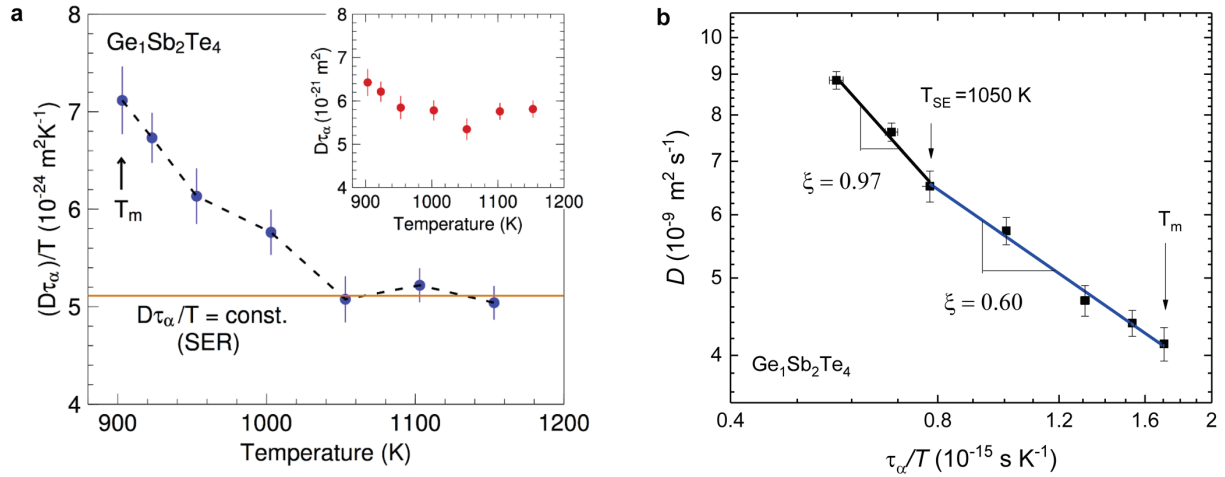


Figure 3. The breakdown of the Stokes-Einstein Relation in liquid PCMs. (a) During cooling, $(D \cdot \tau_\alpha)/T$ initially has a constant value at $T \geq 1050$ K as expected from the SER, but shows a marked positive deviation from the constant below 1050 K as $T_m = 903$ K is approached, indicating a breakdown of the SER at $T_{SE} = 1050$ K. **Inset:** The product $D \cdot \tau_\alpha$ does not exhibit a simple proportionality with temperature and clearly takes on a negative slope at lower temperatures. **(b)** The data fitting with the fractional SER indicates a change of slope from $\xi \approx 0.97 \pm 0.11$ to $\xi \approx 0.60 \pm 0.03$ at $T_{SE} = 1050$ K, as in Fig 3(a).

The breakdown of the SER at such high temperatures ($>T_m$), and short relaxation times, is an important observation, since (i) the SER has provided the basis for calculating viscosity and fragility from simulated self-diffusion coefficients and/or crystal growth velocities (or vice versa) of PCMs near T_m (7, 11, 12), and (ii) it occurs at temperatures where diffusivities are nearly four orders of magnitude higher ($\sim 5 \times 10^{-9} \text{ m}^2 \text{ s}^{-1}$) than where the SER breakdown is observed in conventional glass formers. For instance, for the typical fragile molecular liquid OTP, the SER remains valid down to the much lower diffusivity $D \approx 1.3 \times 10^{-13} \text{ m}^2 \text{ s}^{-1}$ (ref. (30)) where $\eta \approx 7.7 \text{ Pa}\cdot\text{s}$.

Indeed, the observation in $\text{Ge}_1\text{Sb}_2\text{Te}_4$ more resembles the case of the “most anomalous liquid” - supercooled water. For bulk water, the recent data of Dehaoui et al.(31) showed a crossover in the fractional SER behavior from $\xi \approx 1$ at high temperature to $\xi \approx 0.8$ at low temperature. The breakdown temperature T_{SE} of $\sim 340 \text{ K}$, $\sim 1.25T_m$, and the diffusivity $D \approx 5 \times 10^{-9} \text{ m}^2 \text{ s}^{-1}$ at T_{SE} (where viscosity $\eta \approx 0.4 \text{ mPa}\cdot\text{s}$), are comparable to those of $\text{Ge}_1\text{Sb}_2\text{Te}_4$ (see Fig. S4). Note that the deviation from the SER in water appears well above other known anomalies such as density maximum (277 K), rapid C_p increase, and sharp viscosity rising (below T_m). Harris(32), with less extensive data, had earlier reported a SER breakdown in water also at $D = 0.59 \times 10^{-9} \text{ m}^2 \text{ s}^{-1}$ (ref.(33)) with crossover to fractional SE behavior with $\xi=0.67$. As is much discussed, the anomalies of water are thought to be related to a LLT, and possibly a nearby, but hidden, second critical point suggested by some computational models(34).

To further explore the origin of the SER breakdown in such a high-atomic-mobility state of $\text{Ge}_1\text{Sb}_2\text{Te}_4$, we turn to the analogous phenomenology found in some relevant computational models. For instance, in the study of the ‘two-scale’ Jagla ramp potential(35) it was found that a breakdown in the SER began at a temperature of 0.6, which is 50% above the temperature of the Widom line crossing at T_w . Something similar is also observed in models of water, for instance in ST2 water(36), T_x (which is T_{SE} in our case), was found to be $\sim 10\%$ above T_w . Thus, the breakdown itself is not specific to water, but may occur in other systems that possess a liquid-liquid critical point (LLCP). Whether or not the breakdown is due directly to the implied structural heterogeneity is, however, not clear, as the following discussion will emphasize.

As an isobar crosses the ‘Widom-line’ in the supercritical region near the LLCP, the populations of high and low density nanodomains reverse, and response functions like C_p maximize(37). It is natural then to relate the SER breakdown to the critical-point-related structural fluctuations, and the decoupling of viscosity from diffusion behavior(37) that they promote. The

problem we see with this appealing association comes from different sources: two from the simulation literature and the other from our own observations, as follows.

In their detailed study of the SER breakdown in ST2 water, Poole and co-authors(29) concluded that both slow and fast subsets of molecules contributed to the deviation and, furthermore, “the fractional behavior is observed across three distinct physical regimes..., indicating an almost complete insensitivity to changes in the average liquid structure.” Similar conclusions can be reached by analyzing the diffusivity and τ_α data provided for the Fermi-Jagla model in ref.(38) (for results, see SI-Fig.S2). In our own work, we have been struck by the fact that the onset temperature for deviation from the SER occurs in a temperature domain where $S(q,t)$ is still perfectly exponential, with no sign, even at temperatures very near the melting point, of the sort of shoulder usually associated with stretching of the exponential and the development of the dynamic heterogeneity (seen, for instance, in ref.(38) (Fermi-Jagla, see SI)). We note that, however, the MD simulation study of the ISF shows the presence of dynamic heterogeneities in the supercooled GeTe(39), which, originating from structural heterogeneities due to chains of Ge-Ge homopolar bonds, may explain the breakdown of the SER in GeTe in the viscous regime below T_m (40). It is apparently not the case here.

How can we attribute the observed SER breakdown to heterogeneity if, even in the sensitive dynamical properties, we see no sign of heterogeneity? Just as mysterious is the breakdown of SER that we find at temperatures where the relaxation time is so much shorter (ps) than it is in “normal” liquids where SER breakdown occurs e.g. $\tau_\alpha > ns$ for OTP and other glassformers. Is it that the SER is a much more sensitive signaler of impending anomalous character than any of the other signals yet studied? Let us remember that in water the SER breakdown also occurred at picosecond relaxation times.

Given that ‘water-like’ anomalies such as density maxima, and diverging (or peaked) heat capacities, occur in supercooled Te, Ge, Si(41–44), in $Ge_{15}Te_{85}$ just above the eutectic temperature(45), and in As_2Te_3 somewhat above its T_m (46), we should be prepared for unusual behavior in the PCMs at lower temperatures(23). The thermodynamic response function maxima in the above-mentioned chalcogenides are also associated with liquid metal-semiconductor transitions(23). Indeed, pressure-induced polyamorphic transitions between high- and low-density amorphous states (which are also metallic and semiconducting states) have been found in both $Ge_1Sb_2Te_4$ and $Ge_2Sb_2Te_5$ (47–49) and these closely parallel the polyamorphism in amorphous silicon(50) and vitreous ice(51) - except that the latter obviously does not possess a semiconductor-metal transition.

On the basis of all the above, a P - T diagram for liquid, and metastable liquid, states of $Ge_1Sb_2Te_4$ is conjectured in Fig. S5. Its analogy to that of water is provided by the inset. Errington and Debenedetti(52) showed that a “Russian doll” of nested kinetic and thermodynamic anomalies

exists in water and the same has since been found for other water-like systems (e.g. Si and SiO₂(53, 54)). The anomaly persisting to the highest temperature is the structural characteristic related to openness of structure -- or tetrahedrality in the case of water. The figure suggests that, as theorized for water, a metastable critical point might exist not far from ambient pressure in liquid PCMs and not only give rise to the SER breakdown above T_m , but also facilitate crystallization processes below T_m , as has previously been argued for the cases of globular proteins, and some colloidal and Lennard-Jones fluid systems which possess a LLC(55–58). Indeed, Tanaka's two-order-parameter model already predicts that a "V-shape" P - T phase diagram, as is for this PCM case, is directly related to thermodynamic and dynamic anomalies similar to those of water(59). The fact that we observe the same sort of breakdown for PCMs lends credence to the suggested phase diagram even though a proper understanding of the breakdown remains elusive. The proposed scenario of a LLT is supported by the evidence of a fragile-strong crossover/transition found recently in a similar composition Ge₂Sb₂Te₅ below T_m , manifesting as a continuous crossover argued by Chen et al.(15), and as a singular temperature (792 K) argued by Flores-Ruiz et al.(60) by data fitting.

What do the above considerations (assuming their validity) imply for the deeper understanding of PCM function and related future research in this area? Space limitations compel brevity, so we refer to previous discussions of the felicitous effect of a fragile-to-strong transition occurring shortly below T_m , by speeding crystallization on the high temperature side of the peak and arresting the dynamics by a fragile-to-strong transition on passing the peak(23, 24, 45, 61). Urgent for improvement of this understanding is the elucidation of the character of the glasses produced by hyperquenching, and finding their relation to alternative polyamorphs mentioned above. If a first-order transition is involved, then it should be possible to trap the microdomains that coexist transiently during the hyperquench and analyze them by TEM coupled with EDX and related techniques. For continuous transitions, density studies of the glassy phases, trapped by quenching at different rates, should be diagnostic. Glasses made using different sputter schedules, should offer an alternative approach. Acquired data would permit a mapping out of the features of the potential energy hypersurface(62) ("energy landscape"), on which the system is being trapped. Is it a single landscape or is there a discontinuous gap (first-order transition)(63)?

It is important that the phenomena described in this work are not confused with recent reports of SER breakdown above " T_m " (a ternary eutectic temperature) in certain glass-forming metallic mixtures, such as ZrCuAl, where the species Cu decouples from the Zr-Al matrix(64, 65). The latter phenomenon is more closely related to the case of Cu in amorphous silicon, where D_{Cu} can be four orders of magnitude greater than that of the host (Si) atoms(66). A related phenomenon,

also quite different from our conjecture, is the superionicity of Cu (or Ag) cations in many superionic glassformers, where the mobile ion decoupling is observed well above any liquidus temperature, (and also above $2T_g$), and the Stokes-Einstein discrepancy at T_g can reach 11 orders of magnitude(67)).

SUMMARY

We have performed neutron scattering studies of diffusion and relaxation times in the PCM $\text{Ge}_1\text{Sb}_2\text{Te}_4$, and identified a breakdown in the SER well above the T_m - which lies in a relaxation time domain 10^4 times shorter than in normal liquids. We link this to the behavior observed in liquid silicon, germanium, and water, where it is seen as a consequence of a submerged liquid-liquid transition which provokes facile crystallization and fragile-to-strong transitions when ultrafast cooling preserves the liquid state. The exploration of PCMs' anomalous liquid-state behavior will be an essential step towards understanding the fast phase switching behavior in this class of material.

MATERIALS AND METHODS

Sample preparation

$\text{Ge}_1\text{Sb}_2\text{Te}_4$ was prepared using the Ge, Sb, and Te elements with purities ranging from 99.999 to 99.9999 at. %. The elements were sealed under vacuum (10^{-6} mbar) in a fused quartz tube with internal diameter of 5 mm and synthesized in a rocking furnace for homogenization at 900°C for 15 hours.

QENS measurements and data analysis

The sample, sealed in the fused quartz tube, was loaded into a thin-walled Al_2O_3 container for the QENS measurements, which were carried out at the time-of-flight spectrometer TOFTOF at the Heinz Maier-Leibnitz neutron source (FRM II) in Munich(68, 69). Two incident neutron wavelengths $\lambda_i = 4.4$ and 7 \AA were used to obtain a broad q and energy transfer range along with a high resolution of about 90 \mu eV (full width at half maximum).

Spectra were collected as a function of temperature in a high-vacuum high-temperature Nb-furnace. Raw time-of-flight data were normalized to a vanadium standard and interpolated to constant q to obtain the dynamic structure factor $S(q, \omega)$ using the FRIDA-1 software [See <http://sourceforge.net/projects/frida/> for source code.] All spectra were found to be well described

by a model composed of the quasi-elastic scattering from the alloy melt and a flat background to approximate the processes too fast to be accurately measured by the spectrometer. The $S(q, \omega)$ obtained in the measurements where $\lambda_i = 7 \text{ \AA}$ were additionally modeled to include the elastic scattering from the container. In general, the model $S(q, \omega)$ reads:

$$S(q, \omega) = R(q, \omega) \otimes N[A_0 \delta(\omega) + (1 - A_0)L(q, \omega)] + b(q, \omega),$$

where $R(q, \omega)$ is the instrumental resolution function, N is a normalization factor, A_0 is the magnitude of the elastic scattering and $b(q, \omega)$ is a constant but q -dependent, background. The symbol \otimes denotes a numerical convolution. The quasi-elastic scattering was found to be best described with a single Lorentzian of the form (see SI-Fig.S1),

$$L(q, \omega) = \frac{1}{\pi} \frac{\Gamma(q)}{(\hbar\omega)^2 + \Gamma(q)^2},$$

where Γ is the half-width at half-maximum. Below $q^2 \sim 0.6 \text{ \AA}^{-2}$ the incoherent scattering from Ge and Te dominates and the coherent contributions from thermal diffusion (Rayleigh line) and acoustic modes are effectively contained in the flat background of the observed quasi-elastic spectra(70). A mean Ge/Te self-diffusion coefficient was determined via

$$D_{Ge/Te} = \frac{\Gamma(q)}{\hbar q^2}.$$

An analysis was carried out also in the time domain first by obtaining the intermediate scattering function $S(q, t)$ (or density correlation function) via cosine Fourier transform of the measured $S(q, \omega)$ and normalizing to the instrumental resolution function $R(q, t)$. In general, the data were then fitted with a simple exponential decay as

$$S(q, t) / S(q, 0) = f(q) \exp[-t / \tau(q)] + c,$$

where $f(q)$ is the amplitude, τ is the structural relaxation time and the constant c is an offset that takes care of any remaining elastic scattering. It should be noted that this is in line with the model used for $S(q, \omega)$, as the Fourier transform of a Lorentzian is indeed a simple exponential. In order to ensure consistency of the analyses in both energy transfer and time domain, we restricted the fitting range in the energy transfer domain to $[-1, 1]$ meV and in the time domain to the data points after 0.65 ps. At higher energy transfers and shorter times, the spectra are dominated by phononic vibrations and fast relaxation processes. The self-diffusion coefficient was obtained from the time domain analysis via

$$D_{Ge/Te} = \tau(q)^{-1} q^{-2}.$$

The values of $D_{Ge/Te}$ reported in the manuscript represent an average of the values obtained in both analyses.

REFERENCES

1. M. Wuttig, N. Yamada, Phase-change materials for rewriteable data storage. *Nat Mater.* **6**, 824–32 (2007).
2. N. Yamada, E. Ohno, K. Nishiuchi, N. Akahira, M. Takao, Rapid-phase transitions of GeTe-Sb₂Te₃ pseudobinary amorphous thin films for an optical disk memory. *J. Appl. Phys.* **69**, 2849–2856 (1991).
3. K. Shportko *et al.*, Resonant bonding in crystalline phase-change materials. *Nat. Mater.* **7**, 653–658 (2008).
4. W. Zhang *et al.*, Role of vacancies in metal–insulator transitions of crystalline phase-change materials. *Nat. Mater.* **11**, 952–956 (2012).
5. J. Kalb, F. Spaepen, M. Wuttig, Calorimetric measurements of phase transformations in thin films of amorphous Te alloys used for optical data storage. *J. Appl. Phys.* **93**, 2389–2393 (2003).
6. J. A. Kalb, M. Wuttig, F. Spaepen, Calorimetric measurements of structural relaxation and glass transition temperatures in sputtered films of amorphous Te alloys used for phase change recording. *J. Mater. Res.* **22**, 748–754 (2007).
7. J. Orava, L. Greer, B. Gholipour, D. W. Hewak, C. E. Smith, Characterization of supercooled liquid Ge₂Sb₂Te₅ and its crystallization by ultrafast-heating calorimetry. *Nat. Mater.* **11**, 279–83 (2012).
8. C. A. Angell, Formation of glasses from liquids and biopolymers. *Science.* **267**, 1924–1935 (1995).
9. M. D. Ediger, P. Harrowell, L. Yu, Crystal growth kinetics exhibit a fragility-dependent decoupling from viscosity. *J. Chem. Phys.* **128**, 034709 (2008).
10. W. L. Johnson, J. H. Na, M. D. Demetriou, Quantifying the origin of metallic glass formation. *Nat. Commun.* **7**, 10313 (2016).
11. M. Salinga *et al.*, Measurement of crystal growth velocity in a melt-quenched phase-change material. *Nat. Commun.* **4**, 2371 (2013).
12. M. Schumacher *et al.*, Structural, electronic and kinetic properties of the phase-change material Ge₂Sb₂Te₅ in the liquid state. *Sci. Rep.* **6**, 27434 (2016).
13. I. Chang, H. Sillescu, Heterogeneity at the Glass Transition: Translational and Rotational Self-Diffusion. *J. Phys. Chem. B.* **101**, 8794–8801 (1997).
14. G. C. Sosso, J. Behler, M. Bernasconi, Breakdown of Stokes–Einstein relation in the supercooled liquid state of phase change materials. *Phys. Status Solidi B.* **249**, 1880–1885 (2012).

15. B. Chen, G. H. ten Brink, G. Palasantzas, B. J. Kooi, Crystallization Kinetics of GeSbTe Phase-Change Nanoparticles Resolved by Ultrafast Calorimetry. *J. Phys. Chem. C*. **121**, 8569–8578 (2017).
16. A. Meyer, Atomic transport in dense multicomponent metallic liquids. *Phys. Rev. B*. **66**, 134205 (2002).
17. A. Bartsch, K. Rätzke, A. Meyer, F. Faupel, Dynamic Arrest in Multicomponent Glass-Forming Alloys. *Phys. Rev. Lett.* **104**, 195901 (2010).
18. F. Yang, T. Unruh, A. Meyer, Coupled relaxation processes in a glass forming ZrTiNiCuBe liquid. *EPL Europhys. Lett.* **107**, 26001 (2014).
19. J. Brillo, A. I. Pommrich, A. Meyer, Relation between Self-Diffusion and Viscosity in Dense Liquids: New Experimental Results from Electrostatic Levitation. *Phys. Rev. Lett.* **107**, 165902 (2011).
20. C. Bichara, M. Johnson, J. P. Gaspard, Octahedral structure of liquid GeSb₂Te₄ alloy: First-principles molecular dynamics study. *Phys. Rev. B*. **75**, 060201 (2007).
21. C. Steimer *et al.*, Characteristic Ordering in Liquid Phase-Change Materials. *Adv. Mater.* **20**, 4535–4540 (2008).
22. W. Zhang *et al.*, How fragility makes phase-change data storage robust: insights from ab initio simulations. *Sci. Rep.* **4**, 6529 (2014).
23. Shuai Wei, G. J. Coleman, P. Lucas, C. A. Angell, Glass Transitions, Semiconductor-Metal Transitions, and Fragilities in Ge-V-Te (V=As, Sb) Liquid Alloys: The Difference One Element Can Make. *Phys. Rev. Appl.* **7**, 034035 (2017).
24. J. Orava, H. Weber, I. Kaban, A. L. Greer, Viscosity of liquid Ag–In–Sb–Te: Evidence of a fragile-to-strong crossover. *J. Chem. Phys.* **144**, 194503 (2016).
25. A. Tölle, Neutron scattering studies of the model glass former ortho -terphenyl. *Rep. Prog. Phys.* **64**, 1473 (2001).
26. C. Klieber *et al.*, Mechanical spectra of glass-forming liquids. II. Gigahertz-frequency longitudinal and shear acoustic dynamics in glycerol and DC704 studied by time-domain Brillouin scattering. *J. Chem. Phys.* **138**, 12A544 (2013).
27. J. P. Boon, S. Yip, *Molecular Hydrodynamics* (Courier Corporation, 1980).
28. Z. Sun, J. Zhou, A. Blomqvist, L. Xu, R. Ahuja, Local structure of liquid Ge₁Sb₂Te₄ for rewritable data storage use. *J. Phys. Condens. Matter.* **20**, 205102 (2008).
29. S. R. Becker, P. H. Poole, F. W. Starr, Fractional Stokes-Einstein and Debye-Stokes-Einstein Relations in a Network-Forming Liquid. *Phys. Rev. Lett.* **97**, 055901 (2006).

30. F. Fujara, B. Geil, H. Sillescu, G. Fleischer, Translational and rotational diffusion in supercooled orthoterphenyl close to the glass transition. *Z. Für Phys. B Condens. Matter.* **88**, 195–204 (1992).
31. A. Dehaoui, B. Issenmann, F. Caupin, Viscosity of deeply supercooled water and its coupling to molecular diffusion. *Proc. Natl. Acad. Sci.* **112**, 12020–12025 (2015).
32. K. R. Harris, Communications: The fractional Stokes–Einstein equation: Application to water. *J. Chem. Phys.* **132**, 231103 (2010).
33. W. S. Price, H. Ide, Y. Arata, Self-Diffusion of Supercooled Water to 238 K Using PGSE NMR Diffusion Measurements. *J. Phys. Chem. A.* **103**, 448–450 (1999).
34. P. Gallo *et al.*, Water: A Tale of Two Liquids. *Chem. Rev.* **116**, 7463–7500 (2016).
35. L. Xu, H. E. Stanley, Relation between the Widom line and the dynamic crossover in systems with a liquid–liquid phase transition. *Proc Natl Acad Sci.* **102**, 16558–16562 (2005).
36. P. H. Poole, S. R. Becker, F. Sciortino, F. W. Starr, Dynamical Behavior Near a Liquid–Liquid Phase Transition in Simulations of Supercooled Water. *J. Phys. Chem. B.* **115**, 14176–14183 (2011).
37. L. Xu *et al.*, Appearance of a fractional Stokes–Einstein relation in water and a structural interpretation of its onset. *Nat. Phys.* **5**, 565–569 (2009).
38. G. Sun, L. Xu, N. Giovambattista, Relationship between the potential energy landscape and the dynamic crossover in a water-like monatomic liquid with a liquid–liquid phase transition. *J. Chem. Phys.* **146**, 014503 (2017).
39. G. C. Sosso, J. Colombo, J. Behler, E. Del Gado, M. Bernasconi, Dynamical Heterogeneity in the Supercooled Liquid State of the Phase Change Material GeTe. *J. Phys. Chem. B.* **118**, 13621–13628 (2014).
40. S. Gabardi, S. Caravati, G. C. Sosso, J. Behler, M. Bernasconi, Microscopic origin of resistance drift in the amorphous state of the phase-change compound GeTe. *Phys. Rev. B.* **92** (2015).
41. H. Kanno, H. Yokoyama, Y. Yoshimura, A New Interpretation of Anomalous Properties of Water Based on Stillinger’s Postulate. *J Phys Chem B.* **105**, 2019–2026 (2001).
42. S. Sastry, C. A. Angell, Liquid–liquid phase transition in supercooled silicon. *Nat. Mater.* **2**, 739–743 (2003).
43. M. H. Bhat *et al.*, Vitrification of a monatomic metallic liquid. *Nature.* **448**, 787–790 (2007).

44. N. Jakse, A. Pasturel, S. Sastry, C. A. Angell, Response to “Comment on ‘Dynamic aspects of the liquid-liquid phase transformation in silicon’ ” [J. Chem. Phys.130, 247102 (2009)]. *J. Chem. Phys.* **130**, 247103 (2009).
45. S. Wei, P. Lucas, C. A. Angell, Phase change alloy viscosities down to T_g using Adam-Gibbs-equation fittings to excess entropy data: A fragile-to-strong transition. *J. Appl. Phys.* **118**, 034903 (2015).
46. Y. S. Tveryanovich, V. M. Ushakov, A. Tverjanovich, Heat of structural transformation at the semiconductor-metal transition in As₂Te₃ liquid. *J Non-Cryst Solids.* **197**, 235–237 (1996).
47. B. Kalkan, S. Sen, J.-Y. Cho, Y.-C. Joo, S. M. Clark, Observation of polyamorphism in the phase change alloy Ge₁Sb₂Te₄. *Appl. Phys. Lett.* **101**, 151906 (2012).
48. Z. Sun *et al.*, Pressure-induced reversible amorphization and an amorphous–amorphous transition in Ge₂Sb₂Te₅ phase-change memory material. *Proc. Natl. Acad. Sci.* **108**, 10410–10414 (2011).
49. Xu Ming, Yu Zhenhai, Wang Lin, Mazzarello Riccardo, Wuttig Matthias, Reversing the Resistivity Contrast in the Phase-Change Memory Material GeSb₂Te₄ Using High Pressure. *Adv. Electron. Mater.* **1**, 1500240 (2015).
50. P. F. McMillan, M. Wilson, D. Daisenberger, D. Machon, A density-driven phase transition between semiconducting and metallic polyamorphs of silicon. *Nat. Mater.* **4**, 680–4 (2005).
51. O. Mishima, Reversible first-order transition between two H₂O amorphs at ~0.2 GPa and ~135 K. *J. Chem. Phys.* **100**, 5910–5912 (1994).
52. J. R. Errington, P. G. Debenedetti, Relationship between structural order and the anomalies of liquid water. *Nature.* **409**, 318 (2001).
53. M. S. Shell, P. G. Debenedetti, A. Z. Panagiotopoulos, Molecular structural order and anomalies in liquid silica. *Phys. Rev. E.* **66**, 011202 (2002).
54. V. V. Vasisht, J. Mathew, S. Sengupta, S. Sastry, Nesting of thermodynamic, structural, and dynamic anomalies in liquid silicon. *J. Chem. Phys.* **141**, 124501 (2014).
55. P. R. Wolde, D. Frenkel, Enhancement of protein crystal nucleation by critical density fluctuations. *Science.* **277**, 1975–1978 (1997).
56. Yu Chen Shen, David W. Oxtoby, Nucleation of Lennard-Jones fluids: A density functional approach. *J. Chem. Phys.* **105**, 6517–6524 (1996).
57. James F. Lutsko, A dynamical theory of nucleation for colloids and macromolecules. *J. Chem. Phys.* **136**, 034509 (2012).
58. J. Russo, H. Tanaka, The microscopic pathway to crystallization in supercooled liquids. *Sci. Rep.* **2**, 505 (2012).

59. H. Tanaka, Simple view of waterlike anomalies of atomic liquids with directional bonding. *Phys. Rev. B.* **66**, 064202 (2002).
60. H. Flores-Ruiz, M. Micoulaut, From elemental tellurium to Ge₂Sb₂Te₅ melts: High temperature dynamic and relaxation properties in relationship with the possible fragile to strong transition. *J. Chem. Phys.* **148**, 034502 (2018).
61. J. Orava, D. W. Hewak, A. L. Greer, Fragile-to-Strong Crossover in Supercooled Liquid Ag-In-Sb-Te Studied by Ultrafast Calorimetry. *Adv. Funct. Mater.* **25**, 4851–4858 (2015).
62. P. G. Debenedetti, F. H. Stillinger, Supercooled liquids and the glass transition. *Nature.* **410**, 259–267 (2001).
63. C. A. Angell, Glass-Formers and Viscous Liquid Slowdown since David Turnbull: Enduring Puzzles and New Twists. *MRS Bull.* **33**, 544–555 (2008).
64. A. Jaiswal, T. Egami, Y. Zhang, Atomic-scale dynamics of a model glass-forming metallic liquid: Dynamical crossover, dynamical decoupling, and dynamical clustering. *Phys. Rev. B.* **91**, 134204 (2015).
65. R. Soklaski, V. Tran, Z. Nussinov, K. F. Kelton, L. Yang, A locally preferred structure characterises all dynamical regimes of a supercooled liquid. *Philos. Mag.* **96**, 1212–1227 (2016).
66. H. Fritzsche, Ed., *Amorphous Silicon and Related Materials* (WORLD SCIENTIFIC, Singapore, 1989), vol. 1 of *Advances in Disordered Semiconductors*.
67. C. A. Angell, Mobile ions in amorphous solids. *Annu. Rev. Phys. Chem.* **43**, 693–717 (1992).
68. T. Unruh, J. Neuhaus, W. Petry, The high-resolution time-of-flight spectrometer TOFTOF. *Nucl. Instrum. Methods Phys. Res. Sect. Accel. Spectrometers Detect. Assoc. Equip.* **580**, 1414–1422 (2007).
69. W. Lohstroh, Z. Evenson, TOFTOF: Cold neutron time-of-flight spectrometer. *J. Large-Scale Res. Facil. JLSRF.* **1**, 15 (2015).
70. A. Meyer, The measurement of self-diffusion coefficients in liquid metals with quasielastic neutron scattering. *EPJ Web Conf.* **83**, 01002 (2015).
71. C. Otjacques, J.-Y. Raty, J.-P. Gaspard, Y. Tsuchiya, C. Bichara, in *Collection SFN* (EDP Sciences, 2011), vol. 12, pp. 233–245.
72. B. Kalkan, S. Sen, B. G. Aitken, S. V. Raju, S. M. Clark, Negative P-T slopes characterize phase change processes: Case of the Ge₁Sb₂Te₄ phase change alloy. *Phys. Rev. B.* **84**, 014202 (2011).
73. B. Kalkan, S. Sen, S. M. Clark, Nature of phase transitions in crystalline and amorphous GeTe-Sb₂Te₃ phase change materials. *J. Chem. Phys.* **135**, 124510 (2011).

74. H. Kanno, C. A. Angell, Water: Anomalous compressibilities to 1.9 kbar and correlation with supercooling limits. *J. Chem. Phys.* **70**, 4008–4016 (1979).
75. T. Bartels-Rausch *et al.*, Ice structures, patterns, and processes: A view across the icefields. *Rev. Mod. Phys.* **84**, 885–944 (2012).
76. G. Pallares, M. A. Gonzalez, J. L. F. Abascal, C. Valeriani, F. Caupin, Equation of state for water and its line of density maxima down to -120 MPa. *Phys Chem Chem Phys.* **18**, 5896–5900 (2016).
77. V. Holten, M. A. Anisimov, Entropy-driven liquid–liquid separation in supercooled water. *Sci. Rep.* **2**, 713 (2012).

Acknowledgements

The authors acknowledge the beamtime at the TOFTOF instrument operated by FRM II at the Heinz Maier-Leibnitz Zentrum (MLZ), Garching, Germany, and financial support provided by FRM II to perform the QENS measurements. S.W. acknowledges the support from Alexander von Humboldt Foundation Feodor Lynen Postdoctoral Research Fellowship, Place-to-be RWTH Start-Up fund, and the DFG within SFB917. P.L. acknowledges financial support from NSF-EFRI award No. 1640860. C.A.A. acknowledges support from National Science Foundation Research Grant No. CHE-1213265.

SUPPLEMENTARY MATERIALS

Supplemental Figures

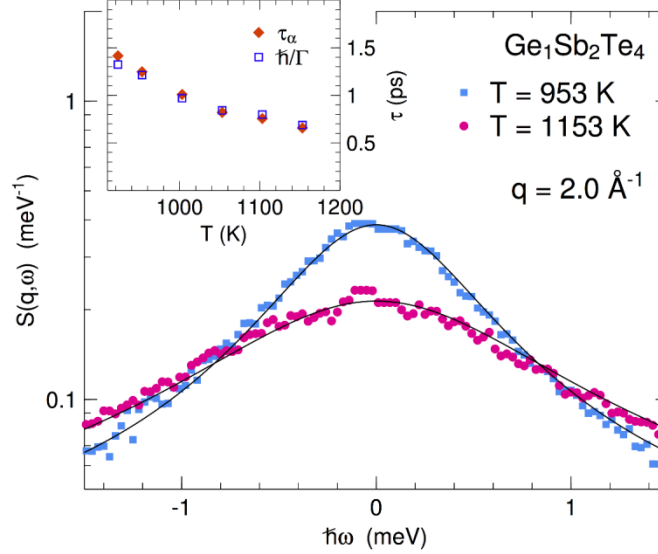


Figure S1. The dynamic structure factor $S(\mathbf{q}, \omega)$ in the energy transfer domain ($\hbar\omega$) obtained from quasi-elastic neutron scattering. The $S(\mathbf{q}, \omega)$ was found to be best described with a single Lorentzian of the form

$$L(q, \omega) = \frac{1}{\pi} \frac{\Gamma(q)}{(\hbar\omega)^2 + \Gamma(q)^2},$$

where Γ is the half-width at half-maximum. The inset shows that the \hbar/Γ values obtained from the energy domain are in good agreement with the τ_α from the analysis carried out in the time domain (see Fig.1a and text), where the intermediate scattering function $S(\mathbf{q}, t)$ is obtained via cosine Fourier transform of the measured $S(\mathbf{q}, \omega)$ and normalized to the instrumental resolution function $R(\mathbf{q}, t)$.

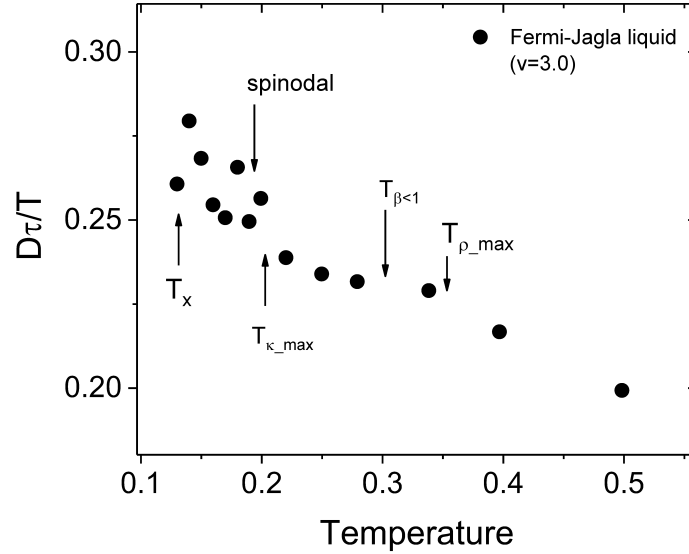


Figure S2. The $D\tau_\alpha/T$ as a function of temperature for the Fermi-Jagla liquid at a volume $v=3.0$ (close to the liquid-liquid critical point volume $v_c \approx 2.9$). Data are adapted from Sun et al. (J. Chem. Phys. 146, 2017). The model liquid exhibits anomalous properties with decreasing temperature. The arrows indicate the temperature of density maximum $T_{\rho_{max}} \approx 0.35$, the onset temperature of the non-exponential decay, $T_{\beta < 1} \approx 0.3$, the temperature of compressibility maximum, $T_{\kappa_{max}} \approx 0.2$, the spinodal line for the liquid-liquid coexistence (close to the critical temperature $T_c \approx 0.18$), and the crystallization temperature $T_x \approx 0.13$. We note that the data of $D\tau_\alpha/T$ show a negative slope as a function of temperature, indicating a violation of the SER within the entire accessible temperature range from 0.5 to T_x . This suggested that the onset of the SER breakdown is likely to be at a higher temperature $T > 0.5$, out of the accessible window. By contrast, the decay of the intermediate scattering functions only become non-exponential at $T_\beta \approx 0.3$ which is even lower than $T_{\rho_{max}}$.

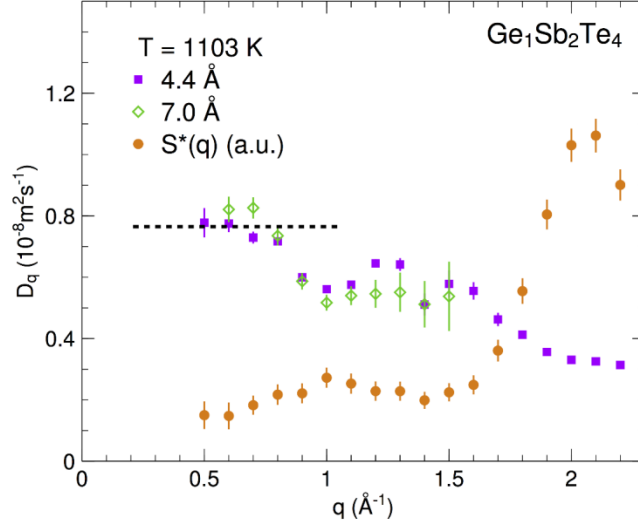


Figure S3. The ‘effective’ diffusion coefficient D_q as a function of q derived at a given temperature of 1103 K using the relation $D_q = 1/(\tau_q q^2)$. The D_q measured at both incoming wavelengths of 4.4 Å and 7 Å are generally in good agreement with each other. The dashed line gives the long-range self-diffusion coefficient in the low- q limit. Integrating the measured $S(q, \omega)$ in an energy transfer range from -0.3 to 0.3 meV yields a quantity $S^*(q)$ similar to the true static structure factor $S(q)$. The reduction in D_q near the main $S^*(q)$ peak at $\sim 2 \text{ \AA}^{-1}$ was predicted by de Gennes (De Gennes, *Physica* 25, 825–839 (1959)), and describes the slowing down of the microscopic dynamics of a liquid in the presence of structural ordering. This feature is also reproduced in the vicinity of the so-called pre-peak in $S^*(q)$ at $q \approx 1 \text{ \AA}^{-1}$, which is indicative of a distinct MRO occurring in liquid $\text{Ge}_1\text{Sb}_2\text{Te}_4$. Note that, as q approaches the pre-peak from lower values, $1/\tau_q$ deviates from the q^2 –dependence, as shown in Fig.2 Inset.

Comparisons of water and GST deviations from the SER

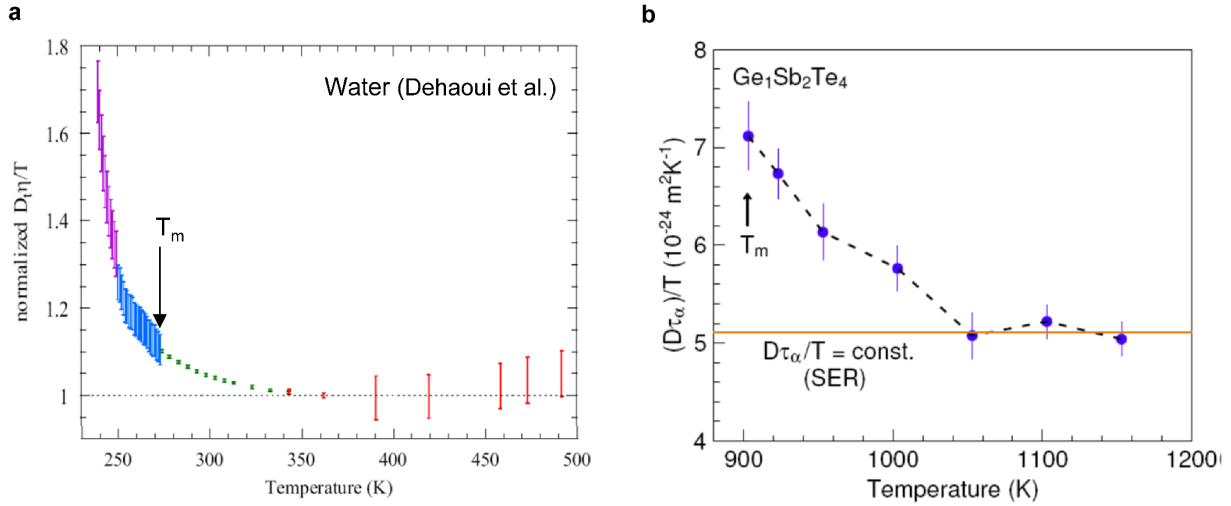


Figure S4. Comparison of the SER breakdown in water (a) [adapted from Dehaoui et al.(31)] and liquid $\text{Ge}_1\text{Sb}_2\text{Te}_4$ (b). The test of the SER in water uses a combined dataset of viscosity η and translational diffusivity D_t with small uncertainties that covers a full temperature range. The sources of the viscosity and translational diffusivity data are given in Table S3 in SI of [31].

Note that the recent study of the SER in water indicates that the liquid deviates from the SER already at around 340 K, which is $\sim 1.25T_m$ and higher than that reported by Harris (258 K). Thus, the breakdown of the SER appears to be the very sensitive early sign of the thermodynamic anomalies that occur at lower temperatures (e.g. density maximum, C_p increase, viscosity rising etc.).

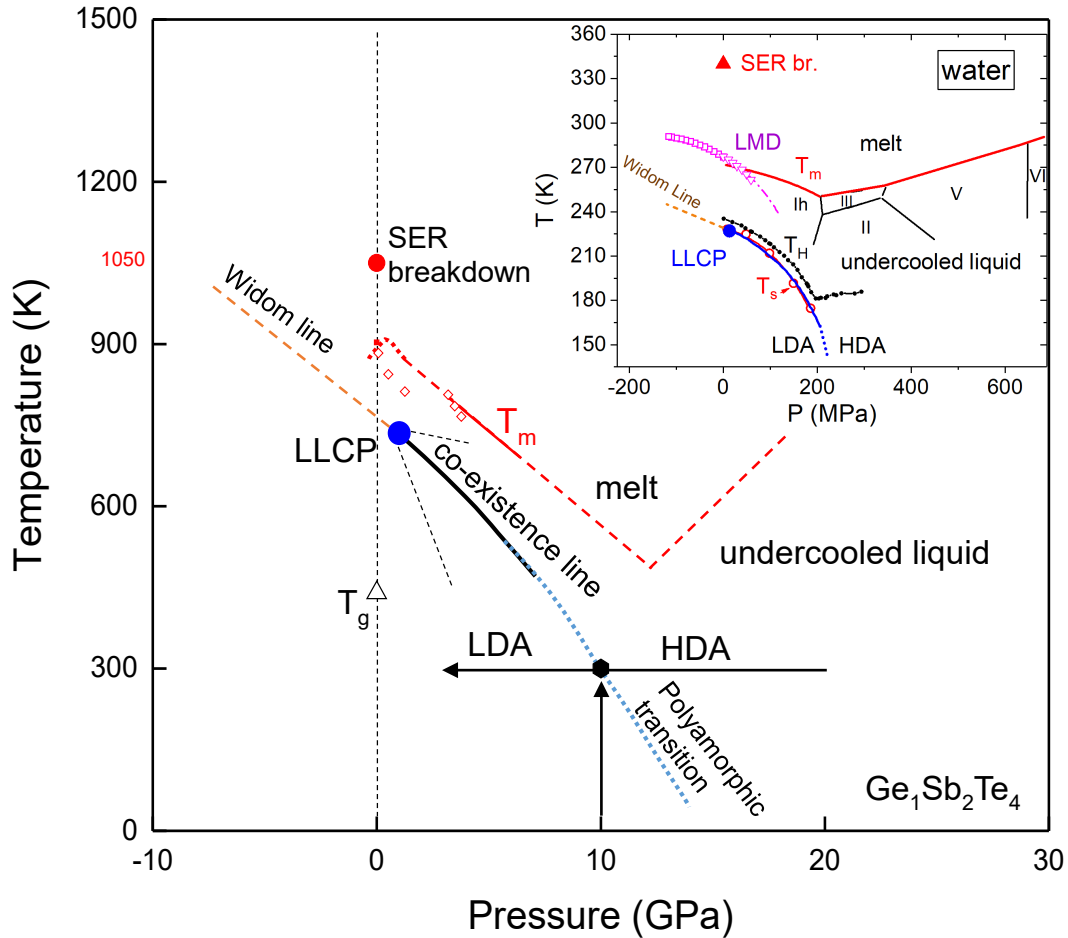


Figure S5. Pressure-temperature (P-T) metastable liquid phase diagram conjectured for $\text{Ge}_1\text{Sb}_2\text{Te}_4$. A liquid-liquid critical point (LLCP) is placed $\sim 30\%$ below the point of the SER breakdown $T_{SE}=1050\text{ K}$, or $\sim 20\%$ below T_m . In the pressure domain, the LLCP is assumed to lie at slightly positive pressure, and under the local T_m -curve maximum. The latter can be justified from the fact that a positive volume change upon melting (i.e. positive Clapeyron slope) is reported(21, 71) at ambient pressure while the high-pressure V-shape T_m -curve (and open diamonds) accords with the work of Sen and coworkers(72, 73). Therefore, the ambient pressure isobar crosses a Widom line (dashed bold line) with a LLCP nearby. At more positive pressures, the speculated liquid-liquid coexistence line has a negative slope to reconcile the negative Clapeyron-slope of the pressure-induced polyamorphic transition (blue dotted line) between high- and low-density amorphous phases (HDA and LDA) of $\text{Ge}_1\text{Sb}_2\text{Te}_4$ at $\sim 10\text{ GPa}$ reported by Kalkan et al.(47). **Inset:** P-T phase diagram of supercooled water. The phase boundaries of melt and ices are taken from ref.(74, 75). The line of maximum densities (LMD) consists of data from an equation of state (open squares) based on sound velocities at negative pressure(76) and data at positive pressure(34) (open triangles), which are supported by extrapolations of the Holten-

Anisimov two-state equation of state (dash-dotted line) up to its stated reliability limit of -100 MPa(77). The SER breaks down in bulk water at ~ 340 K (solid triangle) well above T_m according to Dehaoui et al.(31). T_H is the limit of the homogeneous nucleation temperatures(74). Red open circles and line (T_s) indicate the singular temperatures(74), coinciding with the hypothesized LLCPC and the phase boundary of HDA/LDA water(77).